MODULATION OF INTERNUCLEAR COMMUNICATION IN MULTINUCLEAR RUTHENIUM(II) POLYPYRIDYL COMPLEXES

Wesley R. BROWNE[1], Frances WELDON[2], Adrian GUCKIAN[3] and Johannes G. VOS[4,*]

National Centre for Sensor Research, School of Chemical Sciences, Dublin City University, Dublin 9, Ireland; e-mail: [1] wesley.browne@dcu.ie, [2] frances.weldon@dcu.ie, [3] adrian.guckian@dcu.ie, [4] johannes.vos@dcu.ie

Received May 16, 2003
Accepted June 3, 2003

Dedicated to Professor Sergio Roffia on the occasion of his retirement.

The syntheses and characterisation of a series of mononuclear and dinuclear ruthenium polypyridyl complexes based on the bridging ligands 1,3-bis-[5-(2-pyridyl)-1*H*-1,2,4-triazol-3-yl]benzene, 1,4-bis-[5-(2-pyridyl)-1*H*-1,2,4-triazol-3-yl]benzene, 2,5-bis-[5-(2-pyridyl)-1*H*-1,2,4-triazol-3-yl]thiophene, 2,5-bis-[5-pyrazinyl-1*H*-1,2,4-triazol-3-yl]thiophene are reported. Electrochemical studies indicate that in these systems, the ground state interaction is critically dependent on the nature of the bridging ligand and its protonation state, with strong and weak interactions being observed for thiophene- and phenylene-bridged complexes, respectively.

Keywords: Ruthenium complexes; Mixed valence; LMCT; Spectroelectrochemistry; Cyclic voltammetry; Thiophenes; Pyridines; Triazines; Bridging ligands.

The design and syntheses of polynuclear metal complexes containing electro- and photo-active units is of great interest because of their potential to serve as building blocks for the design of supramolecular assemblies and molecular devices[1]. Ruthenium(II) polypyridine complexes play a key role in the development of systems capable of performing photo- and/or redox-triggered functions, such as charge separation in photochemical solar energy conversion[2] and information storage devices[3]. Especially, species featuring photophysical properties and redox behaviour, which can undergo controlled modification (reversibly) by external stimuli, have received considerable attention[3,4]. One area, which is of considerable interest in this respect, is the control of internuclear interaction in multinuclear assemblies. The role played by the bridging ligand in determining such inter-

action, and in allowing manipulation of its strength by external stimulus, is well recognized[5,6].

In recent years, detailed studies of dinuclear complexes incorporating the 1,2,4-triazole moiety as a bridging unit (*e.g.*, complexes **1a**/**1b** in Fig. 1) have been carried out[7,8]. The 1,2,4-triazolate anion can coordinate directly to

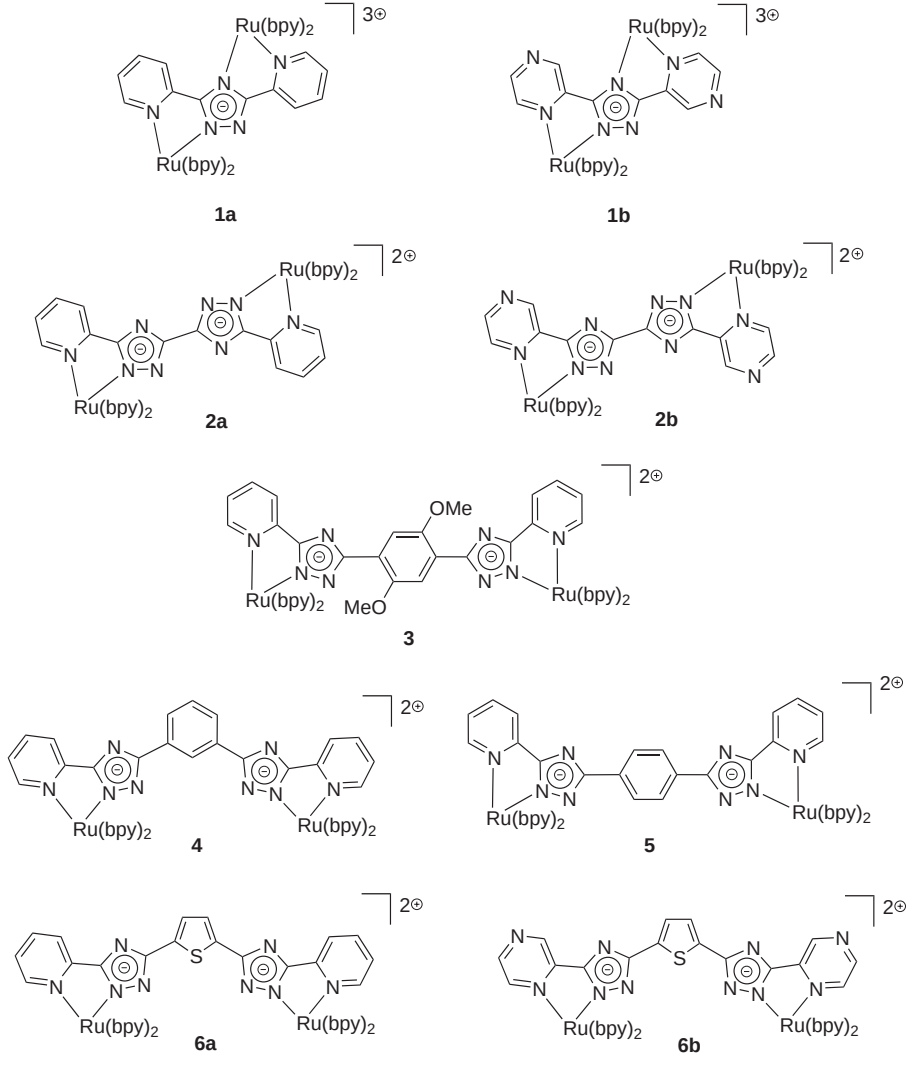

FIG. 1
Dinuclear ruthenium complexes of triazole-based bridging ligands

two metal centres[7,8] (*e.g.*, **1a**) or form a part of an extended bridging unit[9] (*e.g.*, **2a**). The photochemical and photophysical properties of several Rh(III), Ir(III), Ru(II) and Os(II) homo- and heterometallic complexes incorporating 1,2,4-triazole-based bridging ligands, have been extensively studied[8–12]. The results obtained from these studies indicate that interaction between metal centres in dinuclear complexes such as **1a** and **1b** is efficient and facilitated by a hole transfer superexchange mechanism[7e]. More recently, the capability of 1,2,4-triazole-based bridging ligands of tuning the nature of the interaction by variation of both pH and bridging moiety, has been demonstrated in the dinuclear complexes **2a**, **2b** [9] and **3** [12] (see Fig. 1).

In this contribution, the range of triazole-based bridging ligands is expanded (*i.e.*, **4**, **5** and **6a**/**6b**, Fig. 1) in an effort to understand more fully the factors that determine the strength of the ground state interactions in this class of dinuclear complexes. A detailed analysis of the electronic, electrochemical and spectroelectrochemical properties of the dinuclear complexes (Fig. 1) and their mononuclear analogues (Fig. 2) is reported and the results are discussed in the context of earlier studies on related complexes (*i.e.*, complexes **1a**/**1b**, **2a**/**2b** and **3** in Fig. 1)[7–9,12].

RESULTS AND DISCUSSION

Syntheses and Structural Characterisation

The syntheses and structural characterisation of **m4**, **m5**, **4** and **5** (where **m** denotes the mononuclear complex) have been reported elsewhere[13]. Prepa-

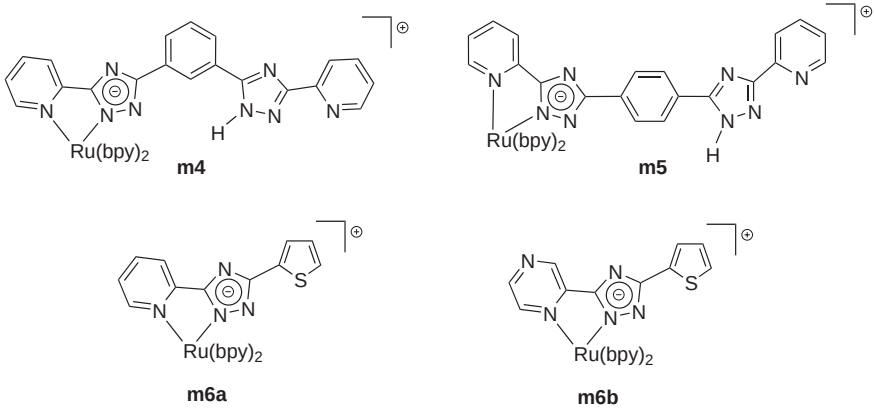

FIG. 2
Mononuclear ruthenium complexes of triazole-based bridging ligands

rations and purification of the dinuclear complexes **m6a**, **m6b**, **6a** and **6b** were carried out by standard procedures, as described in the experimental section. The compounds have been fully characterised by ^{1}H NMR spectroscopy and mass spectrometry. Of particular interest in the previous studies was the formation of coordination isomers, most notably for **2a**/**2b** [9]. For 1,2,4-triazole-based complexes, both N2 and N4 nitrogen atoms of the triazole ring are available for coordination (Fig. 3) resulting, potentially, in the formation of a mixture of isomers, *i.e.*, five dinuclear isomers in the case of **2a** and **2b** [9]. A novel synthetic approach, involving coupling of mononuclear subunits, was employed to successfully prepare **2a**/**2b** with complete control of the coordination mode of the complexes formed[9]. For **4**, **5** and **6a**/**6b**, however, the presence of a bulky substituent in the C5 position of the triazole ring is expected to prevent the formation of N4-bound isomers, based on previous experience with related mononuclear complexes[9,14] and **3** [12]. Hence, direct reaction of the bridging ligands with *cis*-[Ru(bpy)$_2$Cl$_2$] should result in only one major isomer being formed (*i.e.*, where both metal centres are bound *via* the N2 nitrogen).

In order to confirm the coordination mode of the complexes, ^{1}H NMR spectroscopy was employed[12]. Figure 4 shows the ^{1}H NMR spectra of **6a** and its mononuclear analogue **m6a**. The only significant differences between the mononuclear and dinuclear complexes arise from the proton signals due to the spacer group (*e.g.*, the thiophene moiety). For **m6a** signals corresponding to the H3 (d), H4 (dd) and H5 (d) nuclei of the monosubstituted thiophene ring are observed between 7.0 and 7.6 ppm. For **6a** a single resonance at ≈7.45 ppm (2 H) is observed. An additional consideration is the presence of stereoisomers. It would be expected that the dinuclear complexes exhibit twice the number of proton signals due to the presence of diastereoisomers as is the case for **1a** [7d]; however, due to the large separation of the metal centres, no appreciable differences between the ^{1}H NMR spectra of the diastereoisomers are observed. It is clear that the spectra of the mono- and dinuclear complexes are almost identical, confirming that

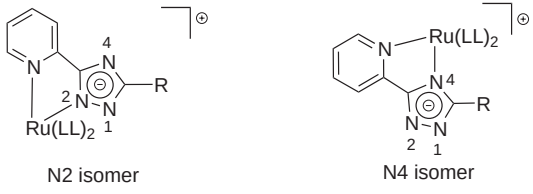

FIG. 3
N2 and N4 coordination modes

the dinuclear complexes are N2–N2 bound, in agreement with related complexes[7,8,12,15]. For **4**, **5** and **6b**, the N2–N2 coordination was confirmed by ^{1}H NMR spectroscopy in a similar manner. For **4**, three phenylene resonances (4 H) are observed, confirming the meta-substitution of the phenylene spacer, whilst for the para-substituted benzene ring of **5**, only a single resonance (4 H) is found. As for **m6a**, in the mononuclear complexes **m4**, **m5** and **m6a**, the loss of symmetry results in an increase in the number of bridging ligand resonances.

Redox Properties

Oxidation and reduction potentials of all complexes together with those for some related systems are presented in Table I. Assignment of the redox processes is accomplished by comparison with previously reported 1,2,4-triazole- and thiophene-containing complexes[7–9,12,16]. The waves in the anodic region of the cyclic voltammograms are assigned to metal-centred and ligand oxidations, while in the cathodic region redox waves are assigned to polypyridyl reductions[23].

Metal-centred oxidation processes. All of the mononuclear complexes exhibit a single metal-centred anodic wave, with both **m6a**/**m6b** and their

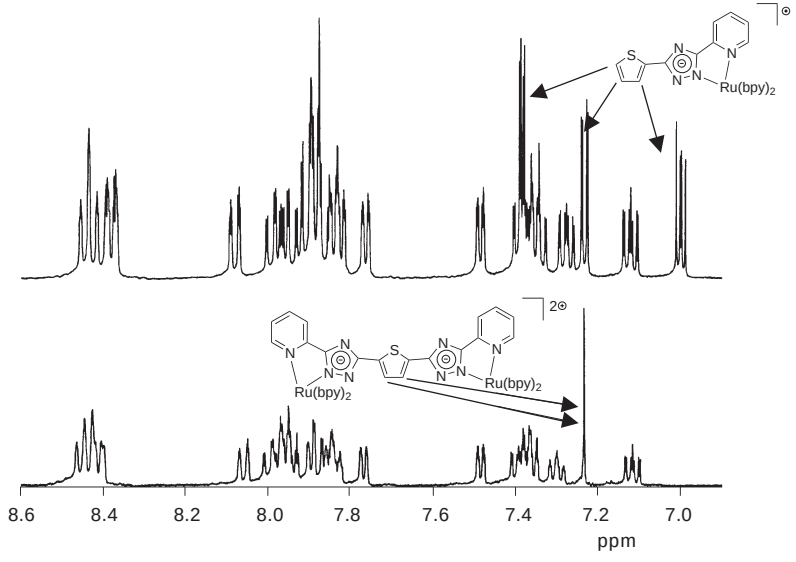

FIG. 4
^{1}H NMR spectra of **6a** (lower) and **m6a** (upper) in CD_3CN

TABLE I
Electronic properties of mono- and dinuclear thiophene-containing complexes (in CH_3CN). The pK_a data for complexes were determined in Britton–Robinson buffer

Comp.	E^{ox}, V[a,c]	E^{red}, V[b,c]	λ_{max}, nm (log ε)	pK_a	Ref.
1a	1.04, 1.34	–1.40, 1.62, –1.67	452	–	7
1b	1.16, 1.46	–1.26, –1.39, –1.55, –1.63	449	–	7
2a	0.80, 0.98	–1.46, –1.72	480	1.1, 3.8	9b
2b	0.92, 1.09	–1.42, –1.65	455	–	9b
3	0.82 (1.20, 1.40)	–1.48, –1.73	481 (4.27)	4.1	12
4	0.84	–1.40, –1.69	482 (2.00)	3.5	–
5	0.84	–1.50, –1.71 (irr)	481 (2.03)	3.6	–
6a	0.78, 0.87 (1.45 irr)	–1.44, –1.67	360 (4.6), 430 (4.23)	2.50	–
6b	0.85, 0.95 (1.41 irr)	–1.49, –1.70	344 (4.33), 438 (4.19), 510 (sh)	1.25	–
m4	0.84	–1.45, –1.60	482 (0.85)	3.3	–
m5	0.84	–1.45, –1.61	482 (0.98)	3.6	–
m6a	0.86 (1.62 irr)	–1.36, –1.67	480 (3.93)	3.05	–
m6b	0.95 (1.55 irr)	–1.43, –1.65	455 (4.15)	2.15	–
H2a	1.06, 1.17	–	440 (4.45)	–	–
H2b	1.09, 1.15	–	436	–	–
$H_2$2a	1.10	–	430	–	9b
$H_2$2b	1.13	–	430	–	9b
$H_2$3	1.25 (1.5)	–1.49, –1.73	412 (4.45)	–	12
$H_2$4	1.18	–1.53	440	–	–
$H_2$5	1.14	–1.52, –1.79 (irr)	420	–	–
$H_2$6a	1.08 (1.45 irr)	not measured	417 (4.45)	–	–
$H_2$6b	1.18 (1.58 irr)	not measured	428, 515 (sh)	–	–
Hm4	1.18	–1.47	440	–	–
Hm5	1.15	–1.47	432	–	–
Hm6a	1.19 (1.67 irr)	–	439 (4.03)	–	–
Hm6b	1.23 (1.55 irr)	–	438 (4.18)	–	–

[a] Ru(II)/Ru(III) couple; ligand oxidation given in parentheses. [b] Ligand reduction. [c] Electrode potential *vs* SCE.

fully protonated forms **Hm6a**/**Hm6b** exhibiting ligand-based oxidation processes (*vide infra*). For the protonated complexes, an anodic shift of 250–300 mV is observed compared with the deprotonated complexes, reflecting the reduction in the σ-donor capacity of the 1,2,4-triazole moiety upon protonation. For the deprotonated dinuclear complexes **4** and **5** and for all fully protonated complexes (*i.e.*, $\mathbf{H_2}$**4**, $\mathbf{H_2}$**5**, $\mathbf{H_2}$**6a** and $\mathbf{H_2}$**6b**) a single two-electron metal-based redox wave (with $\Delta E_p = E_{p,a} - E_{p,c} \approx 70$ mV) is observed, in agreement with the electrochemical properties reported previously for **3** [12]. For the fully deprotonated dinuclear complexes **6a** and **6b**, however, a separation between the first and second metal oxidation waves of approximately 100 mV is observed. This ΔE_p value is close to that observed for the monoprotonated dinuclear complexes **H2a** and **H2b** (Table I)[9].

In multinuclear complexes containing identical, non-interacting centres, a current–potential response having the same redox potential and shape (but increased current) as that of the corresponding molecule containing a single centre is observed[17]. The similarity of the metal redox potentials of the mono- and dinuclear complexes (with the exception of **6a** and **6b**) indicate that electrostatic[18,19] and resonance stabilisation effects are small and, at most, only a small electronic coupling between the two metal centres is present in the ground state[20–22]. The comproportionation equilibrium constant, K_c, is directly related to the difference in the first and second metal oxidation processes (ΔE) and reflects the stability of the mixed-valence complexes (Eq. (*1*)). For **6a** and **6b**, $K_c \approx 60$. For all other dinuclear complexes a statistical value of 4 is assumed since the first and second metal oxidation processes are coincident[23].

$$K_c = e^{\Delta E/25.69} \qquad (1)$$

(ΔE in mV; T = 298 K)

Ligand-centred oxidation processes. As expected, neither **m4**, **m5**, **4** nor **5** exhibit ligand-based oxidation processes[7–10]. For **6a**/**6b** and **m6a**/**m6b**, irreversible oxidation waves arise at *ca* 1.4–1.6 V, assigned as thiophene oxidation. The assignment is based on the redox potentials, irreversibility and comparison with other thiophene-containing complexes[16].

Ligand-centred reduction processes. The reduction waves observed for all the complexes have been assigned as 2,2′-bipyridine (bpy)-based by comparison with structurally related complexes[7,8,10]. The redox waves at *ca* –1.4 and –1.65 V are typical of bpy-based reductions. They occur at more negative

potentials than $[Ru(bpy)_3]^{2+}$ due to the σ donation from the 1,2,4-triazole ligands, which not only increases the electron density at the metal centre, but also enhances back-bonding from the metal to the bpy ligands. The weak interaction between the metal units, indicated by the oxidation behaviour of the dinuclear complexes, is reflected in the reduction patterns observed. In all the dinuclear complexes the first peak is attributed to simultaneous one-electron reduction of a bpy ligand at each metal centre[18]. The electron-rich nature of the thiophene moiety (as indicated by its low oxidation potential) and of the 1,2,4-triazole-based ligands, being weaker π-acceptors than bpy, ensures that they are more difficult to reduce; these redox couples lie outside the potential window investigated. As found for other diimine complexes, irreversible waves corresponding to the second reduction process of the bpy ligands and desorption spikes are observed at negative potentials[24,25]. This situation is particularly aggravated for measurements involving the protonated complexes. As reported previously by Hage[15], it is very difficult to obtain satisfactory reduction potentials in acidic solutions due to adsorption at the electrode surface and deprotonation at negative potentials.

Electronic and Acid/Base Properties of Ru(II) Complexes

The UV-VIS absorption data for all complexes are shown in Table I. The electronic absorption spectra are dominated in the visible region by d_π–π* metal-to-ligand charge transfer (MLCT) transitions typical of complexes of this type[7,8,27]. In the UV region (250–350 nm) the intense absorption bands correspond to ligand-based π–π* transitions associated with the 2,2′-bipyridine and bridging ligands. The UV-VIS absorptions of the deprotonated complexes are all red-shifted with respect to $[Ru(bpy)_3]^{2+}$ as a result of strong σ-donor properties of the negatively charged triazole moiety. Upon protonation, the triazole ring becomes a weaker σ-donor/ stronger π-acceptor, resulting in an overall blue shift in the absorption spectrum. A comparison of the absorption spectra of the mononuclear **m4**/**m5** and dinuclear **4**/**5** complexes in their protonated and deprotonated forms reveals that the energetic positions of the absorption maxima are not significantly different, with the molar absorption coefficients of the dinuclear complexes being twice those of the mononuclear complexes (Table I). For **6a** and **6b**, the situation is complicated by the presence of two absorption bands at *ca* 360 nm and 500 nm which are absent in the spectra of **4** and **5**. These bands are likely to be due to the thiophene group; they were observed previously for terpyridine-based thiophene-bridged systems[16]. Upon

protonation of the coordinated triazole rings, these absorption features are blue-shifted, indicating a destabilisation of the thiophene-based π* energy levels.

The acid dissociation constants (pK_a) for all the novel complexes have been determined from the changes in the absorption spectra of the complexes upon pH variation. For the dinuclear complexes **4**, **5** and **6a**/**6b,** only a single protonation step is observed (Fig. 5). The pK_a values of the complexes (1.25 to 3.3) are found to be strongly dependent on the substituent in the C5 position, in agreement with previous studies[27]. The pK_a values obtained for **m6a**/**m6b** and **6a**/**6b** are lower than those for **m4**, **m5**, **4** and **5**, reflecting the electron-withdrawing character of the thiophene moiety[16]. Similarly, the pyrazine-based complex (**6b**) is more acidic than the analogous pyridine complex (**6a**), due to the greater electron-withdrawing nature of the pyrazine ring[27].

Electronic Properties of Ru(III) Complexes

The spectroscopic features of the Ru(III) complexes are summarised in Table II. Oxidation of the mononuclear complexes results in the disappearance of the MLCT bands and appearance of bands in the region 520–1500 nm. These new bands are assigned as ligand-to-metal charge transfer

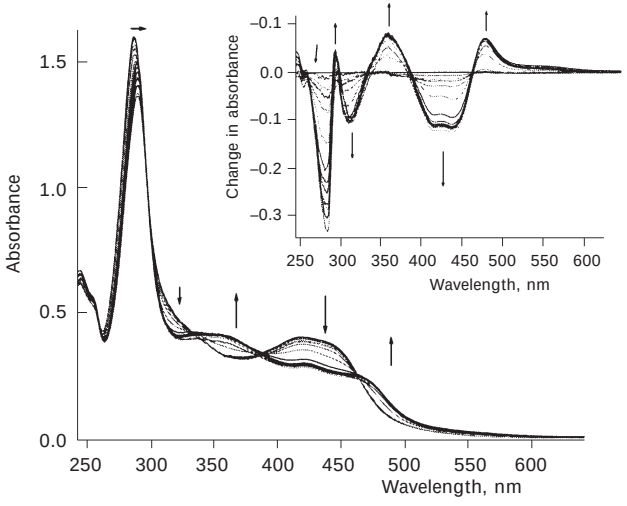

FIG. 5
Changes in UV-VIS spectra of **6b** between pH 0.5 and 10. Inset: difference spectra compared with the completely protonated complexes

(LMCT) bands on the basis of their energetic positions and intensities, and by comparison with structurally related complexes[7e,9,12]. In the UV region, the characteristic splitting and shift to lower energy of the π–π* band (≈280 nm) is indicative of oxidation of metal centres bound to bpy ligands[28]. Clear isosbestic points are obtained in all cases. For **m6a** and **m6b** the oxidation results in the depletion of the absorption bands at *ca* 450 nm, with a concomitant growth in new bands at 425, 569 and 1049 nm. Further oxidation, at potentials above the second (thiophene) oxidation wave, results in an irreversible depletion of all absorption features. For the protonated complexes similar changes were observed, with a slight-blue shift in the energy of the Ru(III) absorption features and a decrease in their intensity (*vide infra*). For the dinuclear complexes similar changes occur in the UV-VIS-NIR spectra upon full (metal-centred) oxidation. For **5**, **6a** and **6b**, however, additional bands are observed during the oxidation process

TABLE II
UV-VIS-NIR absorption data of the fully oxidised ruthenium complexes. All measurements carried out using CH_3CN with 1×10^{-1} M TEAP

Compound	λ_{max}, nm	Compound	λ_{max}, nm	Ref.
1a	725	**1b**		7
2a	570, 910	**2b**	570, 910	9b
H2a	560, 895	**H2b**	560, 895	9b
$H_2$2a	430, 795	**$H_2$2b**	430, 795	9b
3	1216	**$H_2$3**	840	12
m4	530, 923	**Hm4**	520, 850	–
4	525, 927	**H4**	500, 755	–
m5	578, 978	**Hm5**	550, 900	–
5	535, 998	**H5**	537, 870	–
m6a	570, 1050	**Hm6a**	990	–
6a	675, 1310	**H6a**	645, 1270	–
m6b	570, 1060	**Hm6b**	950	–
6b	675, 1320	**H6b**	640, 1265	–

(Fig. 6, *vide infra*). For all compounds complete regeneration of the Ru(II) species was observed, confirming the reversibility of the metal oxidation process.

As can be seen in Table II, the Ru(III) complexes show LMCT bands of varying intensity in the VIS-NIR region[29]. With a few notable exceptions, LMCT absorption bands of Ru(III) complexes have received relatively little attention, in part due to their intensity (*e.g.*, $\varepsilon \leq 500$ l mol^{-1} cm^{-1} for $[Ru(bpy)_3]^{2+}$) and their non-emissive nature. It has been found, however, that both the energy and intensity of LMCT bands can vary greatly[30], with a good correlation between the σ-donor capacity of the ligands and band intensity. Protonation of ligands, which reduces their σ-donor capacity, decreases the intensity of the LMCT bands and increases the energy of the corresponding electronic transitions in comparison with those for the deprotonated complexes[9,12]. LMCT bands of moderate intensities in the red/NIR region were previously observed for mixed-ligand complexes of Ru(III) containing electron-rich donor ligands such as bis(benzimidazole)[31] and 3,5-di(2-pyridyl)-1*H*-1,2,4-triazole (Hbpt)[7e]. The positions and intensities of these LMCT bands correlate well with those reported in this work. The very intense LMCT bands for **m6a**/**m6b** and **6a**/**6b** are, therefore, not unexpected, considering the electron-rich nature of the thiophene group.

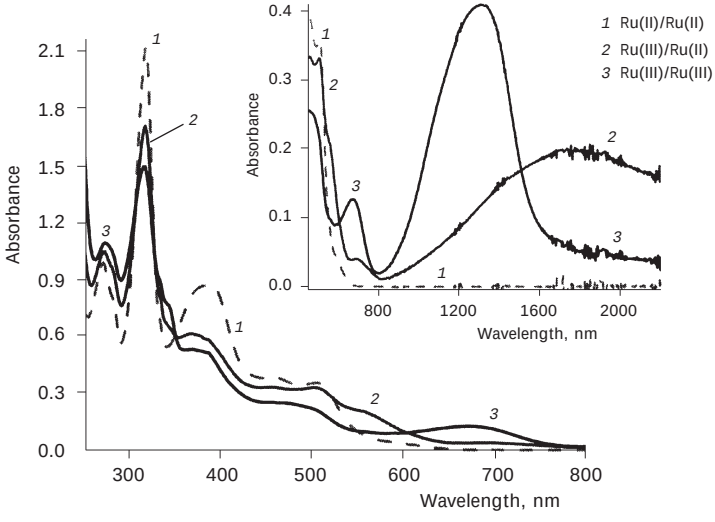

FIG. 6

Changes in UV-VIS absorption spectrum of **6a** upon successive addition of two equivalents of Ce^{4+}. Inset: the NIR region

Electronic Spectroscopy of Mixed-Valence (Ru(II)/Ru(III)) Complexes

Oxidation of the dinuclear complexes results in the progressive decay of the MLCT bands and the concomitant appearance of bands in the red and NIR regions of the spectrum. In the case of **5**, **6a**/**6b** and **$H_2$6a**/**$H_2$6b**, an additional feature appears in the NIR region. Initial oxidation leads to the appearance of an absorption band between 1200 and 2500 nm (Figs 6 and 7). As the oxidation progresses, these bands decrease in intensity and more intense LMCT bands develop at ≈1000 nm. Since these are very similar in energy to those found for the mononuclear parent compounds and persist in the fully oxidised species, they are attributed to a charge transfer from the bridging ligand to the Ru(III) centres. The increase and subsequent decrease of the NIR bands during the oxidation process, together with their position and intensity, strongly suggests[32] that this absorption feature represents an intervalence transition (IT). However, no evidence of such intervalence features can be gathered for **4**. The observation that electronic coupling is not as efficient for meta-substituted aromatic rings, has already been noted by several groups[33–35]. The difference between **4** and **5** in terms of electronic coupling suggests that the interaction can be explained by a hole-transfer superexchange mechanism, since both complexes have similar internuclear separations and, hence, any through-space interactions are expected to be similar.

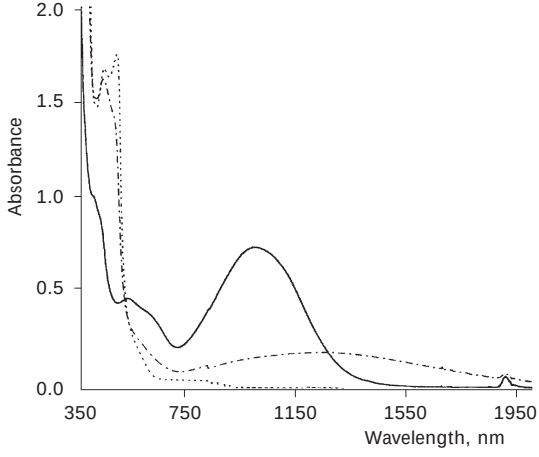

FIG. 7
UV-VIS-NIR absorption spectra of **5** in the Ru(II)/Ru(II) (· · · ·), Ru(III)/Ru(II) (– · – ·) and Ru(III)/Ru(III) (——) oxidation states

The extent of intercomponent interaction is of central importance in the area of supramolecular chemistry. For multinuclear systems that exhibit metal-based redox activity, the most direct method for quantifying the interaction is through electrochemical studies. Whilst K_c may in principle serve as a measure of electronic interaction between two metal sites in a dinuclear complex, it is somewhat limited in identifying the true strength of the electronic delocalisation (α^2) (Eq. (*2*)) and coupling (H_{ab}) (Eq. (*3*)) present. This information can be obtained spectroscopically from the IT bands observed for the mixed-valence complexes, using Eqs (*2*) and (*3*)[36,37].

$$\alpha^2 = 4.2 \times 10^{-4} \left[\frac{\varepsilon_{max} \Delta\nu_{1/2}}{d^2 E_{op}} \right] \qquad (2)$$

$$H_{ab} = \left(\alpha^2 {E_{op}}^2 \right)^{1/2}, \qquad (3)$$

where ε_{max} is the molar absorption coefficient, ν_{max} is the band position in cm^{-1}, $\Delta\nu_{1/2}$ is the band width at half maximum (cm^{-1}) and d is the metal–metal distance in Å. (The relevant spectral parameters obtained from these equations are listed in Table III together with values for related complexes.)

A theoretical basis for the study of IT bands was developed by Hush[38] and by Robin and Day[39], and later by Creutz, Meyer and others[40]. Compared with systems of similar internuclear separation[9,12] (*e.g.*, **2a**/**2b**, **3**), complexes **5**, $\mathbf{H_2}$**6a** and $\mathbf{H_2}$**6b**, show similar coupling strength, while the deprotonated thiophene-bridged complexes (**6a**/**6b**) show considerably increased coupling (Table III). Upon protonation, the IT band moves to a higher energy and is reduced in intensity relative to the LMCT band of the fully oxidised species, indicating a reduction in the level of communication between the metal centres. It should be noted that in the case of the protonated complexes detection of the IT band is very difficult due to its considerable overlap with the much more intense LMCT band. The low energy of the LMCT band is in itself unusual and reflects the reduced energy gap between the ligand HOMO and metal (t_{2g}) orbitals. Examination of Table III shows that protonation reduces the extent of the electronic delocalisation (α^2) by an order of magnitude. However, it should be noted that the degree of electron coupling (H_{ab}) is only moderately reduced. For **6a** and **6b**, the interaction strength, both in terms of delocalisation and coupling for both the protonated and deprotonated complexes, is comparable

TABLE III
Spectroelectrochemical data

Comp.	H_{ab} cm^{-1}	α^2	$\Delta E \pm 10$ mV mV	K_c	d Å[a]	$\Delta\nu_{1/2,calc}$ cm^{-1}	$\Delta\nu_{1/2}$ cm^{-1} [b]	$\varepsilon_{max} \pm 20\%$ l mol^{-1} cm^{-1}	$E_{op} \pm 100$ cm^{-1} cm^{-1}	Ref.
1a	700	0.016	300	117, 910	6.5	2690	3300	2400	5556	7
1b	745	0.019	300	117, 910	6.5	2625	4200	2200	5405	7
2a	459	0.007	180	1, 100	9.5	3060	4690	1820	5490	9b
2b	352	0.004	170	750	9.5	3120	4360	1120	5580	9b
3	480	0.0055	0	4	12	–	5100	>2400	6470	12
5	295	0.0014	0	4	12	–	4262	1040	7870	–
6a	577	0.0102	110	72	11.5	3340	4572	5000	5720	–
6b	565	0.0105	100	50	11.5	3300	4520	5000	5530	–
H2a	435	0.0025	110	72	9.5	4250	5600	1000	8700	9b
H2b	425	0.0025	60	10	9.5	4300	5300	1000	8500	9b
$H_2$6a	444	0.0028	0	4	11.5	–	3430	2600	8400	–
$H_2$6b	430	0.0026	0	4	11.5	–	3400	2600	8450	–

[a] Where X-ray structural data are unavailable, d has been estimated from non-optimised Hyperchem molecular modelling. [b] Taken as double the width at half maximum of the high-energy side of the absorption band. [c] For complexes with a value $K_c \approx 4$, the value of ε_{max} is adjusted to account for concentration[44,45].

to that of **1a** and **1b**. This increased interaction strength may be attributable to the ability of the thiophene HOMO to overlap effectively with both the 1,2,4-triazoles and the metal d-orbitals (as evidenced by the low energy of the LMCT bands), facilitating superexchange interaction[16].

For dinuclear complexes bridged by a single triazole anion, a strong interaction is reflected both in the separation of the first and second metal oxidation waves (ΔE) and in the value of H_{ab} determined from spectroscopic parameters. Separation by two triazole anions shows a decreased level of interaction (*cf.*, **2a**/**2b**). This decrease is due to reduced orbital overlap and, therefore, decreased superexchange-mediated interaction[41]. Inclusion of a phenylene spacer further increases the distance between the metal centres. The level of interaction for these systems (**4** and **5**) is much lower than would be expected on the basis of the increased distance, reflecting the poor ability of benzene groups in mediating interaction[5,42]. For $\mathbf{H_2}$**6a** and $\mathbf{H_2}$**6b** this manifests itself in an increase in the energy of the IT band together with a decrease in its intensity and a reduction in the value of ΔE (see Table III), whilst for $\mathbf{H_2}$**4** and $\mathbf{H_2}$**5** no IT bands were observed. Protonation destabilises both the ligand HOMO and metal t_{2g} orbitals, resulting in a perturbation in the HOMO–t_{2g} orbital overlap. If the mechanism of interaction is *via* hole transfer superexchange, then the perturbation will be manifested by a change in both α^2 and H_{ab}. The electronic coupling factor, H_{ab}, calculated for **5**, is similar to that obtained for the dimethoxy analogue **3** [12]. On the other hand, in compounds, such as **1a** (Fig. 1), where a more direct chemical bond between the metal centres is present, the electronic coupling is considerable stronger, with a H_{ab} value of 700 cm^{-1}. Other cases showing similarly weak coupling as observed for **5** have been reported by Collin *et al.*[42] for dinuclear Ru(II) complexes containing back-to-back bis(terpyridine) ligands linked by phenylene spacers. It could be argued that aromatic groups do not necessarily promote a strong electronic coupling between redox centres. Kim and Lieber found that $(NH_3)_5Ru$ groups connected through dipyridylphenylene units showed very weak intervalence transitions[5]. Ribou and co-workers examined intervalence electron transfer in similar $(NH_3)_5Ru$ complexes of dipyridylpolyenes, dipyridylthiophene and dipyridylfuran and observed stronger, better defined IT transitions than those of the phenylene group. It was suggested that due to its strong aromaticity, phenylene is unfavourable as a mediator of intervalence electron transfer since conjugative interaction with attached units would be realised at the expense of its own aromaticity[43].

Additional information as to the interaction of the metal centres can be obtained by estimation of the theoretical peak width at half height, $\Delta\nu_{1/2,calc}$ using Eq. (*4*)[39].

$$\Delta\nu_{1/2,calc} = [2310(E_{op} - \Delta E)]^{1/2} \qquad (4)$$

If the value of $\Delta\nu_{1/2}$ obtained from this equation correlates well with the value found from direct measurement, the system can be described as valence-localised Ru(II)Ru(III), *i.e.*, Type II. If the IT band is narrower, the system is better described as Type III (valence-delocalised)[39]. On the basis of these data (Table III) and, in particular, since $\Delta\nu_{1/2}$ observed is larger than $\Delta\nu_{1/2,calc}$ it seems clear that the mixed-valence compounds behave as Type II (or valence-trapped) dinuclear species. It is interesting to note that the presence of ancillary groups such as pyrazine or pyridine has little effect on the ground state electronic properties of any of the triazole-bridged systems. The values of ΔE, E_{op} and α^2 obtained for **5a** and **5b** are the same within experimental error (as found previously for **2a** and **2b**)[9]. This observation and the similarity of the energies of the LMCT bands observed for the mixed-valence compounds indicates that the LUMO of the bridging ligand plays, at best, a minor role in determining intercomponent interaction. Instead, it is expected that interaction between the metal centres is taking place *via* a hole transfer mechanism involving the HOMO of the metal units and bridging ligand[5]. This is confirmed by the decreased interaction upon protonation of the bridging ligand. In a hole transfer mechanism, the extent of the interaction depends on the energy-gap between the d_π metal orbitals (metal-based HOMO) and the σ orbitals of the bridge[21]. The spectroscopic and electrochemical data show that the ligand-based σ orbitals are stabilised upon protonation, so that the energy gap between the relevant orbitals *increases*, leading to *decreased* superexchange-assisted electronic interactions.

CONCLUSIONS

As described, the ability to control interaction between metal centres both by external stimuli, such as pH and solvent, and by variation of the spacer group between metal centres is central to the development of molecular devices. One of our aims in recent years has been the investigation of intercomponent interactions in dinuclear compounds with a variety of triazole-based bridging ligands. For compounds based on the different bridging ligands shown in Fig. 1, it was observed that ground state interaction

via hole transfer is strong for **1a**/**1b** but decreases with increasing metal separation. In the phenylene-bridged compounds reported herein, it is evident that the interaction between the metal centres is reduced considerably. The electrochemical data show that the ground-state interaction is much reduced, as expected on increasing the internuclear separation, due to the increasing distance between the metal centres. In addition, since the triazole rings are not coordinated to different metal centres, as observed for **1a** and **1b**, superexchange hole transfer interactions are expected to be reduced. The importance of the hole transfer is further highlighted by the observation that upon protonation of the triazole rings no intervalence bands are observed for **5** and are much weaker for **6a**/**6b**. The behaviour of **4** is quite different, as spectroelectrochemical data do not show any evidence for the presence of an intervalence band. This indicates that apart from distance, electronic coupling effects are important. The absence of an intervalence band is in agreement with the expected reduced electronic coupling for meta- *vs* para-based systems[33–35]. In the systems described above it is clear that the presence of a thiophene spacer allows for a dramatic increase in the distance between metal centres, compared with systems such as **1a** and **1b** with only a relatively minor loss in the interaction strength. In addition, the presence of moieties that allow for external manipulation of the interaction strength, makes these systems much more applicable to the building of supramolecular devices.

EXPERIMENTAL

Materials

All solvents used for spectroscopic measurements were of Uvasol (Merck) grade. All other reagents were HPLC grade or better. The complex *cis*-$[Ru(bpy)_2Cl_2]\cdot 2H_2O$ was prepared by standard procedures[44]. The syntheses and characterisation of **m4**, **m5**, **4** and **5** is reported elsewhere[13].

Instrumentation

^{1}H NMR spectra were recorded on a Bruker AC400 (400 MHz) NMR spectrometer. All measurements were carried out in DMSO-d_6 or $CDCl_3$ for ligands, and CD_3CN for complexes. Chemical shifts are given in ppm (δ-scale). Peak positions are relative to residual solvent peaks. UV-VIS-NIR absorption spectra (accuracy ± 2 nm) were recorded on a Shimadzu 3100 spectrophotometer interfaced with an Elonex PC466 using UV-VIS data manager. Absorption maxima, ±2 nm. Molar absorption coefficients are ±10%. pH titrations were carried out in Britton–Robinson buffer (4×10^{-2} M H_3BO_3, 4×10^{-2} M H_3PO_4, 4×10^{-2} M CH_3CO_2H) (pH was adjusted using concentrated sulfuric acid or sodium hydroxide solution). Mass spectra were obtained using a Bruker–Esquire LC_00050 electrospray ionisation mass spectrometer at

positive polarity with cap-exit voltage of 167 V. Spectra were recorded in the scan range of 50–2200 *m*/*z* with an acquisition time between 300 and 900 μs and a potential between 30 and 70 V. Each spectrum was recorded by summation of 20 scans. Elemental analyses have been carried out at the Micro-analytical Laboratory at the University College Dublin. Electrochemical measurements were carried out on a model 660 Electrochemical Workstation (CH Instruments). Typical complex concentrations were 5×10^4 to 1×10^{-3} mol l^{-3} in anhydrous acetonitrile containing 1×10^{-1} M tetraethylammonium perchlorate (TEAP). Teflon-shrouded glassy carbon working, Pt wire auxiliary and SCE reference electrodes were employed. Solutions for electrochemical reduction measurements were deoxygenated by purging with N_2 or Ar gas for 15 min prior to the measurement. Measurements were made in the range of –2.0 to 2.0 V (*vs* SCE). Protonation of complexes was achieved by addition of 1×10^{-1} M trifluoroacetic acid (in acetonitrile) to the electrolyte solution. Cyclic voltammetric scans were recorded at v = 100 mV s^{-1}; differential pulse voltammetry (DPV) experiments were performed with v = 20 mV s^{-1}, pulse height of 75 mV, and duration of 40 ms. For reversible processes, the half-wave potential values are reported (see Table I); identical values are obtained from DPV and CV measurements. Redox potentials are ±10 mV. Spectroelectrochemistry was carried out using an OTTLE setup comprising of a home-made Pyrex glass, thin layer cell (2 mm). The optically transparent working electrode was made from a platinum/rhodium (90/10) gauze, a platinum wire auxiliary electrode, and an Ag/AgCl pseudoreference electrode. The working electrode was held at the required potential throughout the measurement, using an EG&G PAR model 362 potentiostat. Absorption spectra were recorded as described above. Protonation of complexes under the bulk electrolyses was achieved by addition of dry 1×10^{-1} M trifluoroacetic acid (in acetonitrile).

Syntheses

2-[5-(2-Thienyl)-1H-1,2,4-triazol-3-yl]pyridine (Hpytrth). Thiophene-2-carbonyl chloride (4 ml, 36 mmol) was added dropwise to a stirred solution of Et_3N (4 ml) and pyridine-2-carboximidehydrazide (3 g, 22 mmol) in THF (50 ml). The yellow suspension formed was stirred at room temperature for 2 h, followed by addition of 30 ml of ethanol. The precipitate was collected *in vacuo* and air-dried overnight. The yellow precipitate was heated at reflux in 30 ml of ethylene glycol for 1 h. The solution was then cooled to room temperature. Water (50 ml) was added to the thick off-white suspension. The product was filtered *in vacuo* and recrystallised twice from hot ethanol. Yield 2.5 g (11 mmol, 50%). ^{1}H NMR (400 MHz, DMSO-d_6): 8.73 (1 H, d, pyH6); 8.14 (1 H, d, pyH3); 8.01 (1 H, dd, pyH4); 7.69 (1 H, d, th); 7.65 (1 H, d, th); 7.55 (1 H, dd, pyH5); 7.185 (1 H, dd, th). (Abbreviations: th, thienyl; py, pyridyl; pz, pyrazyl)

2-[5-(2-Thienyl)-1H-1,2,4-triazol-3-yl]pyrazine (Hpztrth). As for Hpytrth, except pyrazine-carboximidehydrazide (3 g, 22 mmol). Yield 1.15 g (5 mmol, 22%). ^{1}H NMR (400 MHz, DMSO-d_6): 9.29 (1 H, d, pzH3); 8.77 (1 H, d, pzH5); 8.76 (1 H, dd, pzH6); 7.74 (1 H, d, th); 7.69 (1 H, d, th); 7.21 (1 H, dd, th).

2,5-Bis[5-(2-pyridyl)-1H-1,2,4-triazol-3-yl]thiophene ((Hpytr)$_2$th). As for Hpytrth, except thiophene-2,5-bis(carbonyl chloride) (prepared by heating 2,5-dicarboxythiophene (1.5 g, 8.7 mmol) in $SOCl_2$ (30 ml) at reflux) was reacted with pyridine-2-dicarboximidehydrazide (3 g, 22 mmol). Yield 674 mg (1.8 mmol, 21%). ^{1}H NMR (400 MHz, DMSO-d_6): 8.74 (1 H, d, pyH6); 8.17 (1 H, d, pyH3); 8.06 (1 H, dd, pyH4); 7.73 (1 H, s, th); 7.57 (1 H, dd, pyH5).

2,5-Bis(5-pyrazinyl-1H-1,2,4-triazol-3-yl)thiophene ((Hpztr)$_2$th). As for Hpytrth, except thiophene-2,5-bis(carbonyl cylchloride) (prepared by heating at reflux of thiophene-2,5-dicarboxylic acid (1.2 g, 6 mmol) in $SOCl_2$ (30 ml) was reacted with pyazinecarboximidehydrazide (2.4 g, 18 mmol). Yield 334 mg (0.9 mmol, 15%). ^{1}H NMR (400 MHz, DMSO-d_6): 9.30 (1 H, d, pzH3); 8.775 (1 H, d, pzH5); 8.765 (1 H, dd, pzH6); 7.61 (1 H, d, th).

[Ru(bpy)$_2$(pytrth)](PF$_6$)·H$_2$O (**m6a**). *cis*-[Ru(bpy)$_2$Cl$_2$]·2H$_2$O (230 mg, 0.44 mmol) and Hpytrth (130 mg, 0.57 mmol) were heated at reflux in 50/50 (v/v) ethanol/water (50 ml) for 8 h. The reaction mixture was evaporated to dryness, redissolved in a minimum of water and filtered to remove unreacted ligand. Three drops of concentrated NH_4OH and 2 ml of saturated aqueous ammonium hexafluorophosphate were added to the filtrate. The precipitate was collected *in vacuo* and air-dried. Purification by column chromatography on neutral alumina (using CH_3CN as eluent) yielded a single red fraction. Solvent was removed *in vacuo* and the precipitate recrystallised from methanol/water. Yield 240 mg (0.31 mmol, 70%). EI MS, *m*/*z*: 640.9 [M$^+$] (for $C_{31}H_{23}N_8RuS$ calculated: 641). ^{1}H NMR (CD_3CN): 8.48 (1 H, d); 8.46 (1 H, d); 8.42 (2 H, d); 8.10 (1 H, d); 8.015 (1 H, dd); 7.98 (1 H, dd); 7.93 (4 H, m); 7.86 (2 H, m); 7.79 (1 H, d); 7.51 (1 H, d); 7.4 (4 H, m); 7.31 (1 H, dd); 7.26 (1 H, d); 7.15 (1 H, dd); 7.03 (1 H, dd). For $C_{31}H_{23}F_6N_8PRuS·H_2O$ (803) calculated: 46.33% C, 2.99% H, 13.95% N; found: 46.32% C, 2.84% H, 13.80% N.

[Ru(bpy)$_2$(pztrth)](PF$_6$)·2H$_2$O (**m6b**). As for [Ru(bpy)$_2$(pytrth)](PF$_6$), except *cis*-[Ru(bpy)$_2$Cl$_2$]·2H$_2$O (230 mg, 0.44 mmol) and Hpztrth (130 mg, 0.56 mmol) were used. Yield 200 mg (0.25 mmol, 57%). EI MS, *m*/*z*: 641.9 [M$^+$] (for $C_{30}H_{22}N_9RuS$ calculated: 642). ^{1}H NMR (CD_3CN): 9.23 (1 H, d); 8.5 (4 H, m); 8.25 (1 H, d); 8.01 (4 H, m); 7.93 (1 H, d); 7.86 (1 H, d); 7.80 (2 H, dd); 7.59 (1 H, d); 7.40 (5 H, m); 7.31 (1 H, d); 7.05 (1 H, dd). For $C_{30}H_{22}F_6N_9PRuS·2H_2O$ (822) calculated: 43.80% C, 2.92% H, 15.33% N; found: 43.60% C, 2.73% H, 15.97% N.

[(Ru(bpy)$_2$)$_2$((pytr)$_2$th)](PF$_6$)$_2$·6H$_2$O (**6a**). As for [Ru(bpy)$_2$(pytrth)](PF$_6$), except *cis*-[Ru(bpy)$_2$Cl$_2$]·2H$_2$O (300 mg, 0.58 mmol) and H$_2$(pytr)$_2$th (100 mg, 0.27 mmol) were heated at reflux in 3/1 (v/v) ethylene glycol/water. Yield 150 mg (0.09 mmol, 36%). EI MS, *m*/*z*: 599 [M^{2+}] (for $C_{58}H_{42}N_{16}Ru_2S$ calculated: 599). ^{1}H NMR (CD_3CN): 8.3 (8 H, m); 7.90 (2 H, d); 7.8 (9 H, m); 7.74 (2 H, d); 7.7 (5 H, m); 7.62 (2 H, d); 7.33 (2 H, d); 7.24 (6 H, m); 7.15 (2 H, dd); 7.08 (2 H, s); 6.97 (2 H, dd). For $C_{58}H_{42}F_{12}N_{16}P_2Ru_2S·6H_2O$ (1596) calculated: 43.66% C, 3.01% H, 14.05% N; found: 43.80% C, 2.77% H, 13.68% N.

[(Ru(bpy)$_2$)$_2$((pztr)$_2$th)](PF$_6$)$_2$ (**6b**). As for [Ru(bpy)$_2$(pytrth)](PF$_6$), except *cis*-[Ru(bpy)$_2$Cl$_2$]·2H$_2$O (290 mg, 0.56 mmol) and H$_2$(pztr)$_2$th (90 mg, 0.24 mmol) were heated at reflux in 3/1 (v/v) ethylene glycol/water (25 ml). Yield 120 mg (0.085 mmol, 33%). EI MS, *m*/*z*: 600 [M^{2+}] (for $C_{56}H_{40}N_{18}Ru_2S$ calculated: 600). ^{1}H NMR (CD_3CN): 9.28 (2 H, d); 8.5 (8 H, m); 8.27 (2 H, d); 8.01 (8 H, m); 7.91 (2 H, d); 7.80 (2 H, m); 7.76 (4 H, d); 7.62 (2 H, d); 7.40 (8 H, m).

We thank Enterprise Ireland for financial support.

REFERENCES

1. a) Worl L. A., Strouse G. F., Younathan J. N., Baxter S. M., Meyer T. J.: *J. Am. Chem. Soc.* **1990**, *112*, 7571; b) Balzani V.: *Tetrahedron* **1992**, *48*, 10443; c) Balzani V., Campagna S., Denti G., Juris A., Serroni S., Venturi M.: *Acc. Chem. Res.* **1998**, *31*, 26; d) Balzani V.,

Scandola F.: *Supramolecular Photochemistry*. Horwood, Chichester 1991; e) Scandola F., Indelli M. T., Chiorboli C., Bignozzi C. A.: *Top. Curr. Chem.* **1990**, *158*, 73.

2. a) Kalyanasundaram K.: *Coord. Chem. Rev.* **1982**, *46*, 159; b) Lehn J.-M.: *Angew. Chem., Int. Ed. Engl.* **1988**, *27*, 89; c) Balzani V., Campagna S., Denti G., Juris A., Serroni S., Ventura M.: *Coord. Chem. Rev.* **1994**, *132*, 1; d) Balzani V., Juris A., Venturi M., Campagna S., Serroni S.: *Chem. Rev. (Washington, D. C.)* **1996**, *96*, 759; e) Slate C. A., Striplin D. R., Moss J. A., Chen P., Erickson B. W., Meyer T. J.: *J. Am. Chem. Soc.* **1998**, *120*, 4885; f) Hu Y.-Z., Tsukiji S., Shinkai S., Oishi S., Hamachi I.: *J. Am. Chem. Soc.* **2000**, *122*, 241; g) Sauvage J.-P., Collin J.-P., Chambron J.-C., Guillerez S., Coudret C., Balzani V., Barigelletti F., De Cola L., Flamigni L.: *Chem. Rev. (Washington, D. C.)* **1994**, *94*, 993; h) Carraway E. R., Demas J. N., DeGraff D. A.: *Anal. Chem.* **1991**, *63*, 332.
3. a) Balzani V. (Ed.): *Supramolecular Photochemistry*. Reidel, Dordrecht 1997; b) Lehn J.-M.: *Supramolecular Chemistry*. Wiley-VCH, Weinheim 1995.
4. a) Beer P. D., Szemes F., Balzani V., Salà C. M., Drew M. G. B., Dent S. W., Maestri M.: *J. Am. Chem. Soc.* **1997**, *119*, 11864; b) Barigelletti F., Flamigni L., Collin J.-P., Sauvage J.-P.: *Chem. Commun.* **1997**, 333; c) Waldmann O., Hassmann J., Müller P., Hanan G. S., Volkmer D., Schubert U. S., Lehn J.-M.: *Phys. Rev. Lett.* **1997**, *78*, 3390; d) Zahavy E., Fox M. A.: *Chem. Eur. J.* **1998**, *4*, 1647; e) Balzani V., Credi A., Venturi M.: *Curr. Opin. Chem. Biol.* **1997**, *1*, 506.
5. Kim Y., Lieber C. M.: *Inorg. Chem.* **1989**, *28*, 3990.
6. Barigelletti F., Flamigni L., Balzani V., Collin J.-P., Sauvage J.-P., Sour A., Constable E. C., Thompson A. M. W. C.: *J. Chem. Soc., Chem. Commun.* **1993**, 942.
7. a) Hage R., Prins R., Haasnoot J. G., Reedijk J., Vos J. G.: *J. Chem. Soc., Dalton Trans.* **1987**, 1389; b) Nieuwenhuis H. A., Haasnoot J. G., Hage R., Reedijk J., Snoeck T. L., Stufkens D. J., Vos J. G.: *Inorg. Chem.* **1991**, *30*, 48; c) Buchanan B. E., Wang R., Vos J. G., Hage R., Haasnoot J. G., Reedijk J.: *Inorg. Chem.* **1990**, *29*, 3263; d) Browne W. R., O'Connor C. M., Villani C., Vos J. G.: *Inorg. Chem.* **2001**, *40*, 5461; e) Hage R., Haasnoot J. G., Nieuwenhuis H. A., Reedijk J., De Rider D. J. A., Vos J. G.: *J. Am. Chem. Soc.* **1990**, *112*, 9245; f) de Wolf J. M., Hage R., Haasnoot J. G., Reedijk J., Vos J. G.: *New J. Chem.* **1991**, *15*, 501.
8. a) Hage R., Dijkhuis A. H. J., Haasnoot J. G., Prins R., Reedijk J., Buchanan B. E., Vos J. G.: *Inorg. Chem.* **1988**, *27*, 2185; b) Barigelletti F., De Cola L., Balzani V., Hage R., Haasnoot J. G., Reedijk J., Vos J. G.: *Inorg. Chem.* **1989**, *28*, 4344.
9. a) Fanni S., Di Pietro C., Serroni S., Campagna S., Vos J. G.: *Inorg. Chem. Commun.* **2000**, *3*, 42; b) Di Pietro C., Serroni S., Campagna S., Gandolfi M. T., Ballardini R., Fanni S., Browne W. R., Vos J. G.: *Inorg. Chem.* **2002**, *41*, 2871.
10. van Diemen J. H., Hage R., Haasnoot J. G., Lempers H. E. B., Reedijk J., Vos J. G., De Cola L., Barigelletti F., Balzani V.: *Inorg. Chem.* **1992**, *31*, 3518.
11. Barigelletti F., De Cola L., Balzani V., Hage R., Haasnoot J. G., Reedijk J., Vos J. G.: *Inorg. Chem.* **1991**, *30*, 641.
12. Passaniti P., Browne W. R., Lynch F. C., Hughes D., Nieuwenhuyzen M., James P., Maestri M., Vos J. G.: *J. Chem. Soc., Dalton Trans.* **2002**, 1740.
13. Weldon F.: *Ph.D. Thesis*. Dublin City University, Dublin 1998.
14. a) Nieuwenhuis H. A., Haasnoot J. G., Hage R., Reedijk J., Snoeck T. L., Stufkens D. J., Vos J. G.: *Inorg. Chem.* **1991**, *30*, 48; b) Fanni S., Keyes T. E., O'Connor C. M., Hughes H., Wang R., Vos J. G.: *Coord. Chem. Rev.* **2000**, *208*, 77.
15. Hage R.: *Ph.D. Thesis*. University of Leiden, Leiden 1991.

16. a) Encinas S., Flamigni L., Barigelletti F., Constable E. C., Housecroft C. E., Scholfield E. R., Figgemeier E., Fenske D., Neuburger M., Vos J. G., Zehnder M.: *Chem. Eur. J.* **2002**, *8*, 137; b) Pappenfus T. M., Mann K. R.: *Inorg. Chem.* **2001**, *40*, 6301; c) Harriman A., Mayeux A., De Nicola A., Ziessel R.: *Phys. Chem. Chem. Phys.* **2002**, *4*, 2229.
17. Flanagan J. B., Margel S., Bard A. J., Anson F. C.: *J. Am. Chem. Soc.* **1978**, *100*, 4248.
18. Giuffrida G., Calogero G., Guglielmo G., Ricevuto V., Ciano M., Campagna S.: *Inorg. Chem.* **1993**, *32*, 1179.
19. Hage R., Haasnoot J. G., Reedijk J., Vos J. G.: *Inorg. Chim. Acta* **1986**, *118*, 73.
20. Curtis J. C., Bernstein J. S., Meyer T. J.: *Inorg. Chem.* **1985**, *24*, 385.
21. Creutz C., Taube H.: *J. Am. Chem. Soc.* **1969**, *91*, 3988.
22. Woitellier S., Launay J.-P., Spangler C. W.: *Inorg. Chem.* **1989**, *28*, 758.
23. Richardson D. E., Taube H.: *Inorg. Chem.* **1981**, *20*, 1278.
24. Cleary R. L., Byrom K. J., Bardwell D. A., Jeffrey J. C., Ward M. D., Calogero G., Armaroli N., Flamigni L., Barigelletti F.: *Inorg. Chem.* **1997**, *36*, 2601.
25. Tokel-Takvoryan N. E., Hemingway R. E., Bard A. J.: *J. Am. Chem. Soc.* **1973**, *95*, 6582.
26. Juris A., Balzani V., Barigelletti F., Campagna S., Belser P., von Zelewsky A.: *Coord. Chem. Rev.* **1988**, *84*, 85.
27. Browne W. R., O'Connor C. M., Hughes H. P., Hage R., Walter O., Doering M., Gallagher J. F., Vos J. G.: *J. Chem. Soc., Dalton Trans.* **2002**, 4048.
28. Milkevitch M., Brauns E., Brewer K. J.: *Inorg. Chem.* **1996**, *35*, 1737.
29. Roffia S., Paradisi C., Bignozzi C. A.: *J. Electroanal. Chem.* **1986**, *200*, 105.
30. a) Nazeeruddin M. K., Zakeeruddin S. M., Kalyanasundaram K.: *J. Phys. Chem.* **1993**, *97*, 9607; b) Kalyanasundaram K., Zakeeruddin S. M., Nazeeruddin M. K.: *Coord. Chem. Rev.* **1994**, *132*, 259.
31. Ohno T., Nozaki K., Haga M.: *Inorg. Chem.* **1992**, *31*, 548.
32. a) Bonvoisin J., Launay J.-P., van der Auweraer M., de Schryver F. C.: *J. Phys. Chem.* **1994**, *98*, 5052; b) Bonvoisin J., Launay J.-P., van der Auweraer M., de Schryver F. C.: *J. Phys. Chem.* **1996**, *100*, 18006.
33. Patoux C., Launay J.-P., Beley M., Chodorowski-Kimmes S., Collin J.-P., James S., Sauvage J.-P.: *J. Am. Chem. Soc.* **1998**, *120*, 3717.
34. Patoux C., Coudret C., Launay J.-P., Joachim C., Gourdon A.: *Inorg. Chem.* **1997**, *36*, 5037.
35. Powers M. J., Meyers T. J.: *Inorg. Chem.* **1978**, *17*, 2955.
36. Creutz C.: *Prog. Inorg. Chem.* **1983**, *30*, 1.
37. Hush N. S.: *Coord. Chem. Rev.* **1985**, *64*, 135.
38. a) Hush N. S.: *Prog. Inorg. Chem.* **1967**, *8*, 391; b) Hush N. S.: *Electrochim. Acta* **1968**, *13*, 1005.
39. Robin M. P., Day P.: *Adv. Inorg. Chem. Radiochem.* **1967**, *10*, 247.
40. Creutz C.: *Prog. Inorg. Chem.* **1980**, *30*, 1.
41. a) Hupp J. T.: *J. Am. Chem. Soc.* **1990**, *112*, 1563; b) Piepho S. B.: *J. Am. Chem. Soc.* **1990**, *112*, 4197; c) Petrov V., Hupp J. T., Mottley C., Mann L. C.: *J. Am. Chem. Soc.* **1994**, *116*, 2171.
42. Collin J.-P., Laine P., Launay J.-P., Sauvage J.-P., Sour A.: *J. Chem. Soc., Chem. Commun.* **1993**, 434.
43. Ribou A.-C., Launay J.-P., Takahashi K., Nihira T., Tarutani S., Spangler C. W.: *Inorg. Chem.* **1994**, *33*, 1325.
44. Richardson D. E., Taube H.: *J. Am. Chem. Soc.* **1983**, *105*, 40.
45. Sutton J. E., Sutton P. M., Taube H.: *Inorg. Chem.* **1979**, *18*, 1017.
46. Sullivan B. P., Salmon D. J., Meyer T. J.: *Inorg. Chem.* **1978**, *17*, 3334.